Enabling Tactical Pursuit-Evasion Game Strategies via Shaping Task Regulation with Coverage Control ⋆

Gregory Hicks * **Xiaotian Xu** ** **Yancy Diaz-Mercado** **

* *AMDS, Johns Hopkins University Applied Physics Laboratory, Laurel, MD 20723, USA (e-mail: gregory.hicks@jhuapl.edu)*
** *Department of Mechanical Engineering, University of Maryland, College Park, MD 20742, USA (e-mail: xxu0116@umd.edu, yancy@umd.edu)*

Abstract: Multi-agent pursuit-evasion games are complex. A practical approach to managing this complexity is through policy that seeks to achieve higher-level game-state objectives via localized tactical tasking of teams of agents working collaboratively. Common tactical tasks are field shaping tasks through which the pursuers exercise influence over the evader in order to alter the state of the game. In this paper we develop the mathematics of field shaping, demonstrate how shaping tasks are defined, and indicate how task performance may be robustly regulated using coverage control. A formal general framework for the conceptual description of shaping tasks is provided. The results are validated in simulation of an example tactical task which regulates pursuers to get in between the evader and its target for different pursuer team sizes.

Keywords: Pursuit-Evasion Games, Tactical Motion Planning, Shaping Tasks, Coverage Control, Multi-agent and Networked Systems, Path Planning and Motion Control, Robotics

1. INTRODUCTION

Multi-agent systems (MASs) may collaboratively tackle complicated tasks that pose challenges for a single agent. Coordination strategies for MASs can be designed based on sensing or communication requirements using techniques such as establishing leader-follower networks as in Hu and Feng (2010) and potential field methods as in Hagelbäck and Johansson (2008). In this paper we approach coordination through coverage control as in Cortés et al. (2002), wherein coordination is achieved by partitioning a domain of interest into regions of dominance (e.g., Voronoi tessellations, as in Arslan and Koditschek (2016)). Coverage control algorithms have been used for achieving human-swarm interaction (Li and Liu (2019)), translation control of MASs (Xu and Diaz-Mercado (2020)), persistent environment monitoring (Lee and Kim (2019)), and pursuit-evasion games (Zhou et al. (2016)). However, collaborative shaping tasks for MASs in adversarial games, which involve strategic deployment of agents to exercise influence over the adversary, have yet to be addressed in the literature.

In this paper we seek to regulate the behavior of a team of agents to shape the playing field of the game. The proposed general concept has profound potential in different tactical tasks of a team of agents, e.g., reach-avoid games (Bhattacharya et al. (2010); Zhou et al. (2012); Davydov et al. (2021)), where it can be used to tackle problems via designing appropriate shape functions and aggregate merit functions that encode game strategies for the pursuer team. We take a tactical task, which regulates pursuers to get *in between* a faster evader and its target, as an example for illustrating the mathematical framework developed. In Fig. 1, a team of blue agents influence the behavior of a red agent that is attempting to reach a target while avoiding capture. Though capture may not be possible, the blue team leverages their influence on the red agent's behavior and shapes the field to pose a challenging obstacle (a non-convex structure) in a tactical fashion.

The main contributions of this paper are threefold: **1)** We provide a formal general framework for the conceptual description of shaping tasks, including the concepts of capture interfaces, shaping merit functions, and gradient-based control strategies. **2)** We propose examples of shaping aggregate merit functions that encode different strategies to deter the evader from its goal. Feeding user-designed merit functions in the proposed general framework would result in different strategic behaviors in pursuit-evasion games. **3)** We analyze a tactical task with the property of in-betweenness and provide a control strategy that regulates to the desired shaping task and a convergence condition based on geometric relationships. The results are verified by simulation over various configurations of pursuer team size.

The organization of this paper is as follows: Section 2 introduces preliminary definitions for shaping tasks. Section 3 provides the general framework of shaping task regulation. Then, a betweenness tactical task design is studied in Section 4 as an example. The simulations and results of the studied pursuit-evasion game are presented in Section 5, and finally the conclusions are drawn in Section 6.

2. DOMAIN SHAPING IN PURSUIT-EVASION GAMES

Our interest is in the following game. We consider an evader e in a convex domain $\Omega \subset \mathbb{R}^n$ with the objective of reaching

⋆ This material is based upon research supported by, or in part by, the U.S. Office of Naval Research under award number N00014-21-1-2410 and a contract from the Johns Hopkins University Applied Physics Laboratory, award number 304791.

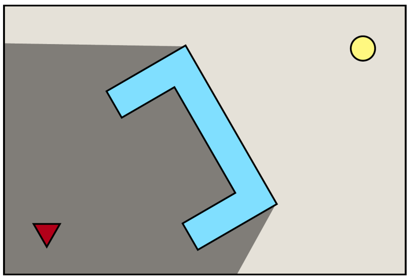

Fig. 1. High-level description of a shaping task. The red agent has to make it to the yellow target while avoiding blue regions (composed of potential capture regions by a team of adversarial agents). One strategy for the blue agents is to create a cul-de-sac (non-convex) shape to induce challenges on the red agent's motion planner and prevent it from reaching its goal or influence its decision making (e.g., steer towards a particular part of the space) in a tactical fashion. The darker region in the space represent the points from which there is no direct path to the goal.

a goal position $g \in \Omega$. The evader is avoiding capture by the N pursuers $\{p_i\}$, $i \in \{1,\ldots,N\} = [N]$. In general, the pursuers win if they (ε-)capture e or spoil its goal-reach objective for a specified time (possibly ∞). Various proper definitions for specific games can be found in Chen et al. (2016) and Rivera-Ortiz et al. (2020).

We assume for all players the steering dynamics $\dot{p}_i = \sigma_i u_i$, $\dot{e} = \sigma_e u_e$, where $\sigma = \|v\|$ denotes speed and $u = \mathrm{vers}(v) = v/\|v\|$ (the versor of v). Here the subscript i indicates a pursuer and e the evader. It follows that the control actions u lie in $\mathbb{S}^{n-1}$, which denotes the unit sphere as an embedded Riemannian manifold of n-dimension Euclidean space.

2.1 Domain Shaping

The Capture Interface Central to the notion of evasion games is that which is to be avoided. Capture, the strict coincidence of a pursuer p_i with the evader e, is to be avoided by e. However, more conservatively, we consider avoidance of the following reachability related set, which mitigates the possibility of capture.

Definition 1. (Agent domain of dominance). For agent p_i, $i \in [N]$, the agent domain-of-dominance is the set $D_i \subset \Omega$ which is reachable by p_i prior to e.

Definition 2. (Agent capture interface). For agent p_i, $i \in [N]$, the agent capture interface Γ_i of p_i is the boundary of its domain-of-dominance D_i.

The agent capture interface is best described implicitly as the 0-level set of the signed distance function $\phi_i : \Omega \to \mathbb{R}$. We will call ϕ_i the agent i's capture function, and define the capture function ϕ by the equation $\phi = \min_i\{\phi_i\}$.

Definition 3. (Capture interface). The capture interface Γ of $\{p_i\}$ is the 0-level set of the capture function ϕ.

The dynamics of the capture interface are given by the level-set partial differential equation

$$\phi_t + \phi_x V\left(p_1, \dot{p}_1, \ldots, p_N, \dot{p}_N, e, \dot{e}\right) = 0 \tag{1}$$

where ϕ_t and ϕ_x are the partial derivatives of ϕ with respect to time and the states of the agents (including p_i and e) respectively, and V is the interface velocity field, which is the time derivative of the interface points extended from Γ appropriately over Ω. We may restrict to $V(p_i, \dot{p}_i, e)$ in (1) to describe the dynamics of ϕ_i for propagation of a component of the larger interface.

The Time-of-Arrival Function We now consider a part of the domain, $G \subset \Omega$.

Definition 4. (Time-of-arrival function). The time-of-arrival function $T_{G;\sigma} : \Omega \to \overline{\mathbb{R}}_{\geq}$ provides the minimum time it takes to travel from $q \in \Omega$ to G in the speed field $\sigma : \Omega \to \mathbb{R}_{\geq}$.

When G and σ are clear from context, or discussion does not depend on their specification, we will drop the use of the subscript and simply write T.

The time of arrival function satisfies the Eikonal equation

$$\|\nabla T\| = 1/\sigma \qquad \text{s.t.} \quad T|_G = 0. \tag{2}$$

The Shape Function The capture function partitions Ω into the half spaces defined by $\Omega^{\geq} = \phi^{-1}(\mathbb{R}_{\geq})$ and $\Omega^{\leq} = \phi^{-1}(\mathbb{R}_{\leq})$, respectively.

Definition 5. (Capture domain). The half-space $\Omega^{\leq}$ is called the capture domain.

We will now couple the level-set equation (1) for the capture interface with the Eikonal equation (2) simply by defining the binary speed field $\sigma_\Gamma = 1\ \forall q \in \Omega^{\geq}$ and 0 otherwise. The associated solution T with σ_Γ to (2) then evolves with Γ (denoted as T_Γ); it provides the minimum 'time-of-arrival'/geodesic distance while avoiding the capture domain. Let us also define the free speed field, $\sigma_0 = 1$, which has associated to it the solution T_0 to (2).

Definition 6. (Shape function(s)). The shape function $S : \Omega \to \overline{\mathbb{R}}_{\geq}$ is defined by $S = T_\Gamma - T_0$, which is difference in time of arrival due to avoiding the capture domain obstacle. In a completely analogous manner we define S_i.

The shape function is the mathematical construct of the notion of domain shaping, which exercises influence and control over a player in the field due to the threat of (but not necessarily true) capture.

3. SHAPING TASK REGULATION

A pursuer can exert an influence on an evader avoiding capture through their capture-interface signed-distance function. For this reason, we can use the field shapes that pursuers achieve to strategically impose on the evader. That is, we have the game dynamics

$$\phi_t + \phi_x V = 0, \quad S_i = h_i\left(\phi_i\right), \quad S = h\left(\phi\right) \tag{3}$$

Intuitively, the pursuer's strategy is impeding the evader if $S(e) > 0$, and the extent of this is proportional to S (e.g., shaded region in Fig. 1). For instance, we strategically break e if $S(e) = \infty$ (for then there are no safe paths to g). To formalize such ideas let us introduce the following implicit, high-level notion of strategy.

Definition 7. (Tactical Task Specification). Let

$$f_e : C^1\left(N_e \subseteq \Omega^{\geq}\right) \to \overline{\mathbb{R}}^n : S \mapsto s.$$

Then a tactical task specification is the tuple (f_e, N_e, s_e) that specifies a component-wise inequality $f_e(S) \succ s_e$.

Our problem is then as follows:

Problem 1. Given a set of pursuer agents $\{p_i\}$ with game dynamics (3), determine $u_i \in \mathbb{S}^{n-1}$, $i \in [N]$, that regulates S satisfaction of the tactical task specification (f_e, N_e, s_e).

Remark: Definition 7 specifies the tactical task as a tuple where the continuously differentiable strategic function f_e (defined over the evader's region N_e) always imposes a "challenge" on the evader's behavioral scheme, to prevent the evader from completing its task (captured by $f_e(S) \succ s_e$). Problem 1 asks whether a control strategy u_i can be found for pursuers such that the tactical task specification tuple is always satisfied (i.e., the pursers can keep impeding the evader).

In the next section, we explore a strategic element task with a scalar-valued f_e, that is, a single objective.

3.1 Shaping Aggregate Merit Functions

With a single objective, there are at least two situations that readily allow us to transition to encoding our strategy as an aggregate objective function, similar to Martinez et al. (2007).

In the first, we are interested in an equality specification $f_e(S) = s_e$. In this case, we may take the least squares route. Consider $g(x) = -x^2$. The composite $g(f_e(S) - s_e)$ then provides a utility function that relaxes our objective within the strategy-distortion aggregate objective

$$\mathcal{H}_{sd} = -\int_{N_e} (f_e(S) - s_e)^2 \varphi(q)\, dq \tag{4}$$

which measures square error (or strategy distortion) in φ, where φ can be a design parameter that depends on the objective of the task. For regulation, this relaxation is appropriate, because in a game in which our task is feasible, we would clearly reach a global maximum by satisfying the strategy specification on the evader region N_e.

In the second, we wish to have $f_e(S) \geq s_e$, where $f_e(S)$ is a scalar function, and consider the circumstance in which f_e produces a utility function in and of itself. Then, we do the best we can in regulating the specification from a greedy margin perspective if we maximize the aggregate objective

$$\mathcal{H}_s = \int_{N_e} f_e(S) \varphi(q)\, dq. \tag{5}$$

Example: Negative enclosing (Boxed Canyon) objective A commonly employed tactical task in defenses, either as a deterrent or as a precursor to a trap, is the formation of a 'boxed canyon' or 'cul-de-sac'. The point of the boxed canyon is to force the evader to run into the pursuers, or to force it to turn around to avoid doing so. For mechanical systems, such as mobile robots, depending on the relative kinematics and inertias involved, it may be possible for the pursuers to use this strategy to force a capture opportunity.

Mathematically speaking, a boxed canyon imposes a negative gradient in S on N_e with respect to the evader goal g. Let $u_{gx} = \mathrm{vers}(x - g)$, the line-of-sight direction from the goal to x. Then $f_{box}(x) := \langle \nabla S(x), u_{gx} \rangle$ captures succinctly whether or not we are boxing in the position x, and our aggregate boxed canyon merit function is

$$\mathcal{H}_{box} = \int_{N_e} f_{box}(S) \varphi\, dq = \int_{N_e} \langle \nabla S(q), u_{gq} \rangle \varphi(q)\, dq \tag{6}$$

Example: Betweenness (Delay) Objective Our final example is also a common tactical task in defenses, and it is simply to delay or stop the evader by cutting off a direct path to its goal. Geometrically speaking, strict betweenness is simply expressed as e-p_i-g iff $\|e - p_i\| + \|p_i - g\| = \|e - g\|$. From a shaping perspective, we need $S_i(e) > 0$ for some i. We increase "in-betweeness" of e and g the larger $S_i(e)$. Yet further, we can collaboratively seek to best enforce this over a larger area by defining $f_{btwn}(x) = S$, producing the associated aggregate betweenness merit function

$$\mathcal{H} = \int_{N_e} S \varphi\, dq \tag{7}$$

3.2 Gradient controllers

Given the shaping aggregate merit function $\mathcal{H}$, we may regulate the scalar shaping task specification (f_e, N_e, s_e) via the gradient proportional controllers defined by $u_i = \mathrm{vers}(\nabla_{p_i} \mathcal{H})$, where they exist, as this gradient regulates to the critical values of $\mathcal{H}$. How far this regulation, or appropriate variations thereof, go in stabilizing specification performance in some sense is to be determined by active and future research. That said, consider that if on the evader side we are likewise greedy in resisting the strategy, so that $u_e = -\mathrm{vers}(\nabla_e \mathcal{H})$, then taking $\mathcal{H}$ as a Lyapunov candidate we have along closed loop motions

$$\dot{\mathcal{H}} = -\sigma_e \|\nabla_e \mathcal{H}\| + \sum_i \sigma_i \|\nabla_{p_i} \mathcal{H}\|. \tag{8}$$

From (8) we note that: **1)** The pursuers can only increase the shaping merit, and therefore task satisfaction, if their speed weighted strategy sensitivities accumulate to a value that exceeds the speed weighted strategy sensitivities to the evader. **2)** Due to the speed weightings, the pursuers can only suffer inferior speed in two ways. Either because the strategy is more sensitive to pursuers, or because there are more pursuers. **3)** If the pursuers succeed in strategy execution, it can only last so long if the evaders are indeed evading, because we will at some moment come sufficiently close to the desired critical value set point, the gradient with respect to the pursuers will begin to vanish, and the pursuer term can no longer maintain the negative definiteness of the Lyapunov function derivative. **4)** But, when the pursuers collaborate, the evader has a 1-to-many confrontation. If we are careful in the coordination design, the evader cannot spoil all pursuers to an equal degree.

Below, we study a case of shaping task regulation.

4. BETWEENNESS IN REACH-AVOID GAMES

We will look further at an agent shaping realization of the betweenness tactical task and aggregate merit function (7).

4.1 Linear shooting (Cartesian Oval) Approximation

For this case-study, we will work in $\mathbb{R}^2$, and take up a linear shooting approximation in the determination of the pursuers' capture interfaces. Analysis under this assumption shows that the capture interface is then the inscribed circle (i.e., incircle) of the Cartesian Oval defined in Garcia and Bopardikar (2021). One can further find that the radius and center of an incircle of the Cartesian Oval are as follows,

$$r_i = \frac{\varepsilon}{1-\alpha^2} + \frac{\alpha}{1-\alpha^2} d_i,\; o_i = \left(1 - \frac{\varepsilon\alpha + d_i}{d_i(1-\alpha^2)}\right) e + \frac{\varepsilon\alpha + d_i}{d_i(1-\alpha^2)} p_i. \tag{9}$$

Here r_i is a half of the diameter of the Cartesian Oval, which is colinear with the vector $p_i - e$, and o_i its center; $d_i = \|p_i - e\|$; ε

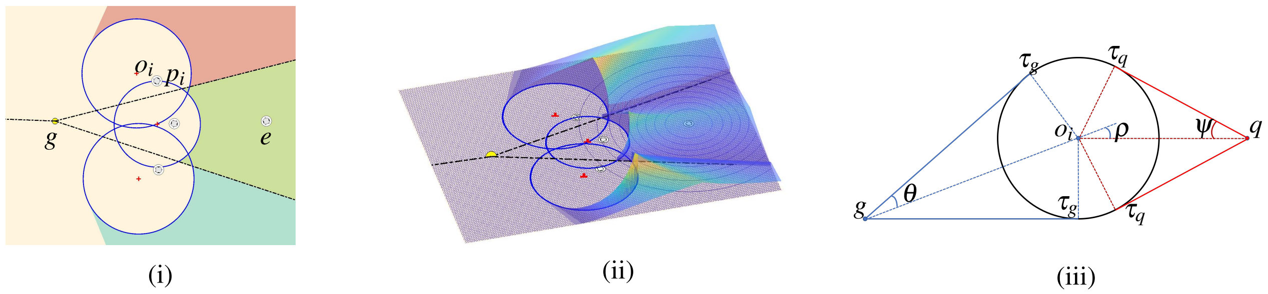

Fig. 2. (i) Geometric illustration of Voronoi tessellation and non-zero support (different color shaded regions) of the shape function $S_i(g, o_i, q)$. (ii) Voronoi tesselation and relation to agent shape functions. The evader on the right wishes to reach the yellow target on the left while avoiding the blue circles which define the pursuers' capture interfaces. The dashed lines define the projective partition of the space into regions of dominance for the pursuers relative to the goal. The 3D surface encodes the magnitude of the shaping function, which casts a shadow on the evader based on the capture interface and its positioning between the goal and evader. (iii) Geometry of the quantities involved in the calculation of the shape function $S_i(g, o_i, q)$.

is a fixed finite distance (e.g., footprint of a robot) for the notion of ε-capture, which is defined as $d_i(t) \leq \varepsilon$ for a prescribed period of time; and $\alpha = \sigma_i/\sigma_e$. We assume the same σ_i, $\forall i$, though they need not be.

In the context of the above discussion we have the agent interface velocity, $\dot{x} = V = \dot{r}N + \dot{o}$, where $N = \nabla\phi/\|\nabla\phi\|$, and ϕ_i is a right circular cone in $\mathbb{R}^3$, which we will call the Cartesian-Oval-incircle cone. The rates $\dot{o}$ and $\dot{r}$ correspond, respectively, to lateral translation of the cone and its vertical, out of plane, motion. The incircle of the Cartesian Oval is the 0-level set of the Cartesian-Oval-incircle cone.

Consistent with the Eikonal equation used in geometric optics, we may imagine the goal g to be a light source emitting light rays. The Cartesian Oval incircle for pursuer p_i blocks the light, and induces a wedge-shaped shadow behind it with 'magnitude' S_i (see Fig. 2(i) & (ii)). Denote the shadowed region, i.e., non-zero support of S_i, by W_i.

4.2 Betweenness Merit Function Revisited

Projective Space and Voronoi Tessellation To induce collaboration between agents in a team, we partition the working space into domains of dominance for each agent. The "dominance" is in the projective angular space $\mathbb{S}^1$. Formally, the angular Voronoi tessellation is defined as

$$V_i(o_i, o_j) = \{q \in \Omega \,|\, |\angle(q, g, o_i)| \leq |\angle(q, g, o_j)|, \forall j\} \quad (10)$$

An agent j is considered as a Voronoi neighbor of agent i if $\partial V_{ij} = V_i \cap V_j \neq \emptyset$, i.e., the shared boundary has non-zero $(n-1)$-dimensional measure (e.g., line segments in $2d$). We denote the agent i's neighbor set as $\mathcal{N}_i$. Thus, each agent has 2 neighbors ($\mathrm{card}(\mathcal{N}_i) = 2$), and only determines its behavior based on the information inside its own dominating area, V_i, and the shared boundary, ∂V_{ij}, with its two neighbors.

Tessellated form We now move to the following agent-based tessellated form of the betweenness merit function

$$\mathcal{H}(\{p_i\}, e) = \sum_{i=1}^{N} \int_{V_i} S_i(q, p_i, e)\varphi(q, e)\,dq \quad (11)$$

where $\{V_i\}$ is the above Voronoi partitioning of the working space Ω, and $\bigcup V_i = \Omega$.

Shape function For a line segments $\overline{pq}$ with endpoints p and q, denote the vector $v_{pq} = q - p$, its length $l_{pq} = \|v_{pq}\|$. From Fig. 2 (iii), it is clear that the length from the goal position g to a point q (the shorter one of two paths) is given by $L_{gq} = l_{g\tau_g} + s_{\tau_g\tau_q} + l_{\tau_q q}$. We take it as obvious that line segments of tangency form right angles with radii, and that the circular arc portion of the geodesic $s_{\tau_g\tau_q}$ runs between the respective points of tangency, τ_g and τ_q. With the Definition 6 of shape functions, we have

$$S_i(q, p_i, e) = L_{gq} - l_{gq}. \quad (12)$$

We are interested in δS_i in terms of the game elements δo_i and δr_i (in turn dependent on δp_i and δe), and these variations will be used for implementing the control strategy, which will be introduced later on (e.g., (13) and (14)). The analytic expressions of these variations can be obtained from the trigonometric relationships and inherent geometry relationships associated with Cartesian Oval incircle and bisectors of the Voronoi tessellation. We omit these expressions due to page constraints, but it will not affect the delivery of the main idea of this paper, i.e., providing and demonstrating a conceptual framework of shaping tasks.

4.3 Dynamic Analysis

As stated previously, with the objective function (11), the agents strategize their behaviors based on the gradient of $\mathcal{H}$. From the chain rule one can get

$$\frac{\partial \mathcal{H}}{\partial p_i} = \frac{\partial \mathcal{H}}{\partial o_i}\frac{\partial o_i}{\partial p_i} + \frac{\partial \mathcal{H}}{\partial r_i}\frac{\partial r_i}{\partial p_i}, \quad (13)$$

$$\frac{\partial \mathcal{H}}{\partial e} = \sum_{i=1}^{N}\left(\frac{\partial \mathcal{H}}{\partial o_i}\frac{\partial o_i}{\partial e} + \frac{\partial \mathcal{H}}{\partial r_i}\frac{\partial r_i}{\partial e}\right) + \frac{\partial \mathcal{H}}{\partial \varphi}\frac{\partial \varphi}{\partial e}. \quad (14)$$

We again omit the explicit expressions of all the components in (13) and (14), but they can be obtained for implementation of the control strategy through geometric relationships and variational analysis mentioned previously.

Lemma 1. (Boundedness of Aggregate Objective). The aggregate strategic objective function (11) is bounded by some constant $C > 0$ if the integrating domain is bounded, and the selected measure function is bounded.

Now let us investigate how the control strategy affects the aggregate strategic objective.

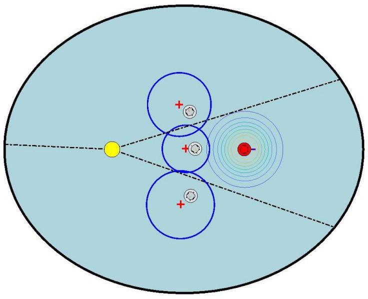

(i) Visualization, $t = 1$ [s]

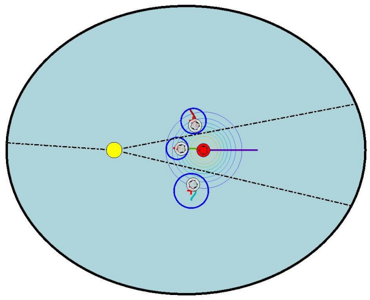

(ii) Visualization, $t = 5$ [s]

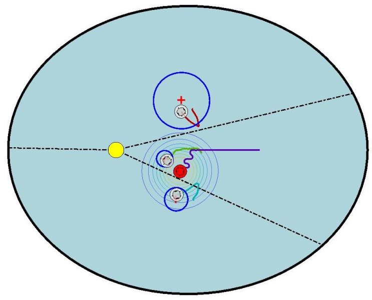

(iii) Visualization, $t = 10$ [s]

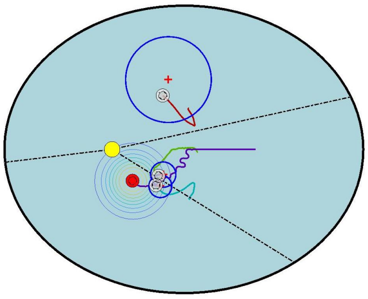

(iv) Visualization, $t = 15$ [s]

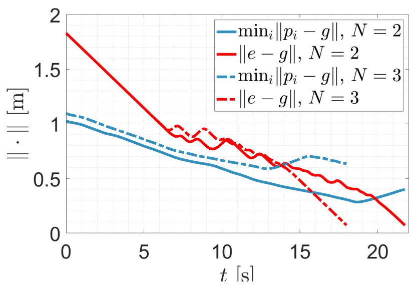

(v) Data Profile, $N = 2$ & 3

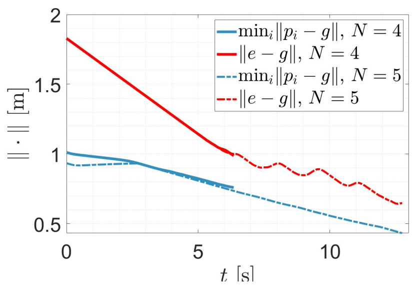

(vi) Data Profile, $N = 4$ & 5

Fig. 3. The visualization of a simulation scenario with $N = 3$ pursuers and "AP+G2G" strategy for the evader. The information of incircles of Cartesian oval, tessellation, trajectories, etc., are visualized at different time instants, i.e., (i)-(iv). In (v) and (vi), the time profile of distances between pursuers and the goal and between the evader and the goal under "AP+G2G" are plotted.

Theorem 1. (System Performance). With the control strategy for pursuer team $\dot{p}_i = \sigma_i u_{p_i} = \sigma_i \text{vers}(\nabla_{p_i}\mathcal{H})$, and for the evader $\dot{e} = \sigma_e u_e = -\sigma_e \text{vers}(\nabla_e \mathcal{H})$, the p_i and e approach to the largest invariant set $M \subset \Omega$, and the system reaches the (local) maximum of (11) as $t \to \infty$ when

$$\sum_{i=1}^{N} \alpha \left\| \frac{\partial \mathcal{H}}{\partial p_i} \right\| \geq \left\| \sum_{i=1}^{N} \left(\frac{\partial \mathcal{H}}{\partial o_i} - \frac{\partial \mathcal{H}}{\partial p_i} \right) + \frac{\partial \mathcal{H}}{\partial \varphi} \frac{\partial \varphi}{\partial e} \right\| \tag{15}$$

Proof. Let us consider $V = -\mathcal{H} + C$, where $C > \mathcal{H}$ follows from Lemma 1, be a Lyapunov candidate of our pursuer system. As we discussed before, $\dot{p}_i = \sigma_i \text{vers}(\nabla_{p_i}\mathcal{H})$, and $\dot{e} = -\sigma_e \text{vers}(\nabla_e \mathcal{H})$, then

$$\begin{aligned}
\dot{V} &= -\sum_{i=1}^{N} \frac{\partial \mathcal{H}}{\partial p_i}\dot{p}_i - \frac{\partial \mathcal{H}}{\partial e}\dot{e} = -\sum_{i=1}^{N} \sigma_i \left\| \frac{\partial \mathcal{H}}{\partial o_i}\frac{\partial o_i}{\partial p_i} + \frac{\partial \mathcal{H}}{\partial r_i}\frac{\partial r_i}{\partial p_i} \right\| \\
&\quad + \sigma_e \left\| \sum_{i=1}^{N} \left(\frac{\partial \mathcal{H}}{\partial o_i}\frac{\partial o_i}{\partial e} + \frac{\partial \mathcal{H}}{\partial r_i}\frac{\partial r_i}{\partial e} \right) + \frac{\partial \mathcal{H}}{\partial \varphi}\frac{\partial \varphi}{\partial e} \right\| \\
\dot{V} &= \sigma_e \Bigg(-\sum_{i=1}^{N} \alpha \left\| \frac{\partial \mathcal{H}}{\partial o_i}\frac{\partial o_i}{\partial p_i} + \frac{\partial \mathcal{H}}{\partial r_i}\frac{\partial r_i}{\partial p_i} \right\| \\
&\quad + \left\| \sum_{i=1}^{N} \left(\frac{\partial \mathcal{H}}{\partial o_i} - \frac{\partial \mathcal{H}}{\partial o_i}\frac{\partial o_i}{\partial p_i} - \frac{\partial \mathcal{H}}{\partial r_i}\frac{\partial r_i}{\partial p_i} \right) + \frac{\partial \mathcal{H}}{\partial \varphi}\frac{\partial \varphi}{\partial e} \right\| \Bigg)
\end{aligned} \tag{16}$$

with $\frac{\partial o_i}{\partial e} = I - \frac{\partial o_i}{\partial p_i}$ and $\frac{\partial r_i}{\partial e} = -\frac{\partial r_i}{\partial p_i}$ from (9).

Enforcing $\dot{V} \leq 0$ yields the condition (15). From LaSalle's theorem (Theorem 4.4 in Khalil (2002)), let E be the set of all points in Ω where $\dot{V} = 0$, then every solution starting in Ω approaches the largest invariant set $M \subset E$ as $t \to \infty$. □

In the condition given by (15), because the summation on the first term is outside the norm, unlike the second term, increasing the number of pursuers could lead to a net decrease in the rate. Herein, we considered the evader always follows the best strategy to maximize (11), which is the worst situation for the team of pursuers. When the evader executes different behaviors, e.g., approaching the goal directly, the trajectory the evader takes should put less burden on pursuers.

5. SIMULATION RESULTS

The shaping task regulation is demonstrated via simulation on teams of varying number of pursuers. The measure φ is taken to be the Gaussian $\varphi(q) = 2\pi \exp\left(-\|q - e\|^2 / (2\sigma^2)\right)$, which concentrates importance around the evader's position. Table 1 provides several metrics for pursuer teams of 2, 3, 4, and 5 agents. The evader implements two different motion planners: (i) avoiding pursuers by turning at a stochastic angle when pursuers are approached while simultaneously going to the goal ("AP+G2G"), and (ii) going to the goal directly. For (i), the evader dynamics are given by

$$\dot{e} = \sigma_e \text{vers}\left((1 - \lambda) R(\theta_e) \left(-\frac{\partial E}{\partial e}^T \right) + \lambda (g - e) \right) \tag{17}$$

where $E = \kappa \sum_{i=1}^{N} (\|p_i - e\| - \varepsilon)^{-2}$, $\kappa > 0$, is an energy-like function whose negative gradient direction drives the evader to avoid the pursuers; $R(\theta_e) = [\cos\theta_e \;\; -\sin\theta_e; \sin\theta_e \;\; \cos\theta_e]$, $\theta_e \in (-\pi/2, \pi/2)$ is a rotation matrix that makes the evader rotate by a uniformly sampled random angle as it gets close to a pursuer; and $\lambda \in (0, 1)$ is a blending coefficient combining the two objectives. For (ii), $\lambda = 1$.

The working space is defined as an ellipse with width 5.1816 [m] and height 3.6576 [m]. The initial distance between the goal and evader is 1.8288 [m], and $\sigma_i = 0.055$ [m/s] $\forall i$ and $\sigma_e = 0.15$ [m/s] (i.e., $\alpha = 2.73$). The $\varepsilon = 0.1$ [m] while the diameter of the robot is 0.14 [m].

Fig. 3 (i)-(iv) illustrates several time instances of a simulation with 3 pursuers for the AP+G2G strategy. It can be seen that the pursuers are back-peddling towards the goal to maximize the objective function (maintaining betweenness) by trying to enlarge the Cartesian Oval incircles. This maintains the capture interface as "obstacles" that influence (delay) the evader's behavior. Additionally, we can see that the Cartesian Oval incircles get, close but maintain some level of separation due to the Voronoi boundary terms between pursuers repelling each other. The level of responsibility to get between depends on the distance to the evader, and the amount of evader measure in the pursuer's cell, though even far away pursuers receive some level of influence. During the simulation, some of the pursuers become unable to maintain betweenness due to the kinematic disadvantage. In these cases, the pursuers that are still able to get in-between gain more responsibility, for example, the two pursuers in the bottom in Fig. 3 (iii), (iv). The terminating condition is that the evader either reaches the goal, or is captured by pursuers. Fig. 3 (v)-(vi) shows the minimum distance between any pursuer and the goal, as well as the distance between the evader and goal, for the AP+G2G evader control strategy and varying number of pursuers. It can be seen in (v) that the pursuers are able to remain in-between the goal and evader as long as the evader distance (red) is above the pursuer distance (blue), however the evader is eventually able to escape and reach the goal. In (vi), enough pursuers are present to maintain in-betweenness for the entirety of the simulation, until the evader is captured.

The operating time $\tau_{\text{operating}}$ of the games, and the time periods of pursuers stay between the evader and the goal $\tau_{\text{inbetween}}$, are recorded in Table 1. We note that as the evader approaches the goal directly (i.e., G2G) with superior speed, but as it is not avoiding the pursuers, the pursuers are able to get in-between the evader and the goal from their initial configuration, and maintain in-betweenness until capture. When the evader employs an avoidance strategy (i.e., AP+G2G), though the pursuers tend to stay between the evader and the goal, capture is less likely due to the evader's superior dynamic capability. However, the evader's approach is influenced by the capture interface, which tactically delays its overall approach. E.g., compared to the time for evader to get to the goal directly ($\tau = 12.2$ [s]), the time for the evader to reach the goal are 21.7 [s] and 18.0 [s] in the simulations with $N = 2$ & 3 pursuers. On the other hand, the slower mobility disadvantage of pursuers can be compensated by increasing the size of the pursuer team, as indicated in the cases of $N = 4$ & 5, where the evader is blocked, and capture is achieved (i.e., $\%_{\texttt{delay}} = 100$).

6. CONCLUSIONS

A general framework of shaping tasks is proposed, and this framework is used for an in-betweenness task in a pursuit-evasion game by specifying the shape and merit functions.

Table 1. Simulation results under different cases. Two strategies of evader are employed, i.e., "AP+G2G" and "G2G." Capture is always achieved in "G2G," and when there is 100% delay.

Evader's Strategy	Estimate Metrics	No. of Pursuers			
		$N=2$	$N=3$	$N=4$	$N=5$
"AP+G2G"	$\tau_{\text{operating}}$	21.7 [s]	18.0 [s]	7.7 [s]	12.8 [s]
	$\tau_{\text{inbetween}}$	19.8 [s]	13.9 [s]	7.7 [s]	12.8 [s]
	$\%_{\text{delay}}$	91.2%	77.2%	100%	100%
"G2G"	$\tau_{\text{operating}}$	6.35 [s]	7.25 [s]	7.4 [s]	7.75 [s]
	$\tau_{\text{inbetween}}$	6.35 [s]	7.25 [s]	7.4 [s]	7.75 [s]

The dynamic analysis of this particular task is presented. The decentralized strategy drives a team of pursuers collaboratively to maintain betweenness, even the evader is kinematically overwhelming, and the evader's planner is agnostic to pursuers. The findings are verified in simulations over various configurations of pursuer teams and different evader behaviors.

REFERENCES

Arslan, O. and Koditschek, D.E. (2016). Voronoi-based coverage control of heterogeneous disk-shaped robots. In *2016 IEEE International Conference on Robotics and Automation (ICRA)*, 4259–4266. IEEE.

Bhattacharya, S., Paul, G., and Sanyal, S. (2010). A cops and robber game in multidimensional grids. *Discrete Applied Mathematics*, 158(16), 1745–1751.

Chen, M., Zhou, Z., and Tomlin, C.J. (2016). Multiplayer reach-avoid games via pairwise outcomes. *IEEE Transactions on Automatic Control*, 62(3), 1451–1457.

Cortés, J., Martinez, S., Karatas, T., and Bullo, F. (2002). Coverage control for mobile sensing networks: Variations on a theme. In *Mediterranean Conference on Control and Automation*, 9–13. Lisbon, Portugal Lisbon, Portugal.

Davydov, A., Rivera-Ortiz, P., and Diaz-Mercado, Y. (2021). Pursuer coordination in multi-player reach-avoid games through control barrier functions. In *2021 American Control Conference (ACC)*, 3222–3227. IEEE.

Garcia, E. and Bopardikar, S.D. (2021). Cooperative containment of a high-speed evader. In *2021 American Control Conference (ACC)*, 4698–4703. IEEE.

Hagelbäck, J. and Johansson, S.J. (2008). Using multi-agent potential fields in real-time strategy games. In *Seventh International Conference on Autonomous Agents and Multi-agent Systems (AAMAS), 12-16, 2008, Estoril*, 631–638.

Hu, J. and Feng, G. (2010). Distributed tracking control of leader–follower multi-agent systems under noisy measurement. *Automatica*, 46(8), 1382–1387.

Khalil, H.K. (2002). *Nonlinear systems; 3rd ed.* Prentice-Hall.

Lee, S. and Kim, Y. (2019). Distributed persistent coverage control and performance evaluation of multi-agent system. *The Aeronautical Journal*, 123(1268), 1701–1723.

Li, W.T. and Liu, Y.C. (2019). Human-swarm collaboration with coverage control under nonidentical and limited sensory ranges. *Journal of the Franklin Institute*, 356(16), 9122–9151.

Martinez, S., Cortes, J., and Bullo, F. (2007). Motion coordination with distributed information. *IEEE control systems magazine*, 27(4), 75–88.

Rivera-Ortiz, P., Diaz-Mercado, Y., and Kobilarov, M. (2020). Multi-player pursuer coordination for nonlinear reach-avoid games in arbitrary dimensions via coverage control. In *2020 American Control Conference (ACC)*, 2747–2753. IEEE.

Xu, X. and Diaz-Mercado, Y. (2020). Multi-agent control using coverage over time-varying domains. In *2020 American Control Conference (ACC)*, 2030–2035. IEEE.

Zhou, Z., Takei, R., Huang, H., and Tomlin, C.J. (2012). A general, open-loop formulation for reach-avoid games. In *2012 IEEE 51st IEEE conference on decision and control (CDC)*, 6501–6506. IEEE.

Zhou, Z., Zhang, W., Ding, J., Huang, H., Stipanović, D.M., and Tomlin, C.J. (2016). Cooperative pursuit with voronoi partitions. *Automatica*, 72, 64–72.